CHEMISTRY
A EUROPEAN JOURNAL

DOI: 10.1002/chem.200700480

Visible Light Induced Catalytic Water Reduction without an Electron Relay

Leonard L. Tinker, Neal D. McDaniel, Peter N. Curtin, Courtney K. Smith, Michael J. Ireland, and Stefan Bernhard*[a]

Abstract: Protons from water are reduced by a catalytic system composed of a heteroleptic iridium(III) photosensitizer $[Ir(ppy)_2(bpy)]^+$, platinum catalyst, and sacrificial reductant. The hydrogen quantum yield reaches 0.26 in this study, which proceeds via reductive quenching of the excited photosensitizer by triethanolamine. This simplified approach allows the characterization of degradation products that are otherwise obscured in more complex systems. A novel 16-well setup for parallel kinetic analysis of H_2 evolution enables high-throughput screening of reaction conditions and quantization of the decaying reaction rate. DFT calculations rationalize the differences between this and previous studies on tris-diimine ruthenium(II) photosensitizers.

Keywords: energy conversion · hydrogen evolution · iridium · photocatalysis · photochemistry

Introduction

The photoinduced cleavage of water using visible light is under intense investigation with the aim to develop an efficient method for converting solar radiation into a convenient and sustainable fuel. There are numerous approaches to achieving this goal, including the use of photovoltaic cells to drive electrolysis,[1] semiconductor-based charge separation techniques,[2–4] thermochemical disproportionation,[5] and the use of catalytic systems that include light-harvesting transition-metal complexes.[6,7] Transition-metal complexes have a distinct advantage over their semiconductor counterparts as their photophysical properties can be "tuned" through ligand modification. Aided by this versatility, researchers have devised a variety of catalytic systems capable of performing the reduction half-reaction of water cleavage, in which the excited state of the transition-metal complex is quenched by charge transfer to an electron relay. Early works report the successful use of $[Ru(bpy)_3]^{2+}$ (bpy = 2,2′-bipyridine) as a photosensitizer, in combination with an electron relay species, and typically employ a platinum catalyst.[8,9] More recent variations involve the attachment of a photosensitizer to TiO_2-supported platinum particles,[10,11] as well as the use of different photosensitizers such as Zn^{II} porphyrins,[12–14] Mg-chlorophyll-*a* from *Spirulina*,[15,16] and cyclometalated $[Ir(C^N)_2(N^N)]^+$ complexes.[17,18]

As a consequence of greater ligand-field stabilization energy (LFSE), the use of cyclometalated Ir^{III} complexes avoids the thermal population of, and subsequent non-radiative decay from, the dissociative ^3MC state observed with tris-diimine Ru^{II} complexes.[19] In addition, the greater energetic requirements for the population of the ^3MC state allow a larger range of excited state energies by altering the ligand architecture.[20] The "tuning" of the $[Ir(C^N)_2(N^N)]^+$ complex's excited state properties is further facilitated by the formation of a mixed excited triplet state associated with metal-to-ligand charge transfer (MLCT) and ligand-centered (LC) transitions linked to the ancillary and cyclometalating ligands, respectively.[21–23]

To facilitate the transfer of reducing equivalents, an electron relay such as methyl viologen is typically employed. The choice of an electron relay is generally crucial to the success of a system; a good relay oxidatively quenches the excited photosensitizer, thereby creating charge separation at the cost of reducing the system's free energy. Numerous relays have been used in place of methyl viologen, including a variety of quaternary bipyridines[24,25] as well as several cobalt[26–28] and rhodium[8,29–31] complexes. Other alternatives include bridged systems where a photosensitizer is covalently linked to a hydrogen evolving metal complex.[32–35] Aside from net energy loss, the use of an electron relay allows

[a] L. L. Tinker, N. D. McDaniel, P. N. Curtin, C. K. Smith, M. J. Ireland, Dr. S. Bernhard
Department of Chemistry, Princeton University
Princeton NJ 08544 (USA)
Fax: (+1) 609-258-6746
E-mail: bern@princeton.edu

Supporting information for this article is available on the WWW under http://www.chemeurj.org/ or from the author.

charge separation at the expense of simplicity, which is compounded by the presence of a sacrificial electron donor that allows hydrogen evolution without concurrent water oxidation. The complexity of such systems hinders the determination of which components are deteriorating and why the catalytic cycle eventually fails.

Herein, we report the first iridium-based catalytic system that uses only a molecular photosensitizer (PS), colloidal metal catalyst, sacrificial reductant, and visible light to evolve substantial amounts of hydrogen in the absence of an electron relay species. Such electron relay deficient systems, while advantageous, are uncommon in the literature.[36] We have previously shown that unlike $[Ru(bpy)_3]^{2+}$, heteroleptic cyclometalated iridium(III) complexes, such as the $[Ir(ppy)_2(bpy)]PF_6$ (Figure 1) (ppy = 2-phenylpyridine) photosensitizer used in this study, are directly quenched by triethanolamine (TEOA).[17] We have found that quenching of the PS creates an activated reduced species capable of independently reducing protons or delivering reducing equivalents to a catalyst to evolve hydrogen. Such a system that avoids an electron relay is inherently simpler and thus easier to study. In addition, energy losses and back reactions associated with the electron transfer to the relay are eliminated, while coupling of the PS to the water redox couple is facilitated. The simplicity of this approach, in combination with our novel photoreactor that dynamically monitors catalytic activity, has made possible the study of degradation products and reaction kinetics. Through such analysis, we have gained insight into the mechanism of hydrogen evolution and this in turn has led us to develop a more robust system.

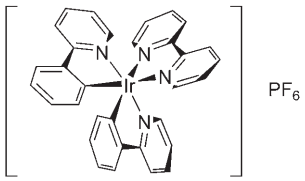

Figure 1. Three-dimensional representation of the $[Ir(ppy)_2(bpy)]$ PF_6 complex used as a photosensitizer in this report.

Results and Discussion

Samples were prepared from PS and K_2PtCl_4 stock solutions in a 9:3:1 acetonitrile/water/TEOA reaction media. After deoxygenating, the samples were illuminated from the bottom, and bubble formation is observed within several minutes. The resulting evolved gas was brought to ambient pressure and analyzed by gas chromatography, or using a calibrated H_2 sensor.

Net hydrogen production with variable [PS] and [K_2PtCl_4]: For comparison to previous studies utilizing this PS with an electron relay,[17] PS and K_2PtCl_4 concentrations were varied to evaluate their effect on net H_2 evolution after 20 h (Figure 2). Minimal hydrogen evolution occurs in the absence of the platinum catalyst (Figure 2B, ■) and hydrogen production is optimal when 0.3 μmol of K_2PtCl_4 is added to the reaction mixture, providing 3400 turnovers per K_2PtCl_4 (Figure 2A). The maximum PS turnover of 15 (using 6.25 μmol PS) is comparable to that with analogous systems that integrate a $[Co(bpy)_3]^{2+}$, $[Rh(bpy)_3]^{3+}$, or methyl viologen electron relay.[9,17,31] H_2 production decreases at greater concentrations of K_2PtCl_4, which cannot be offset by increasing [PS]. In fact, hydrogen evolution is most dramatically diminished at high catalyst and PS loading. This behavior has been ascribed to the faster aggregation of the in situ generated colloidal platinum catalyst[8] of which the particle size has been shown to be strongly correlated to hydrogen evolution in similar systems.[37] A dark solid was generally observed to precipitate from solution during these experiments, which is hypothesized to be the aggregated platinum catalyst. Further examination utilizing a stabilized platinum colloid is described later in this report. For a given $[K_2PtCl_4]$, net hydrogen production was found to be directly proportional to the initial [PS] (Figure 2B), suggesting that the catalytic cycle becomes PS limited.

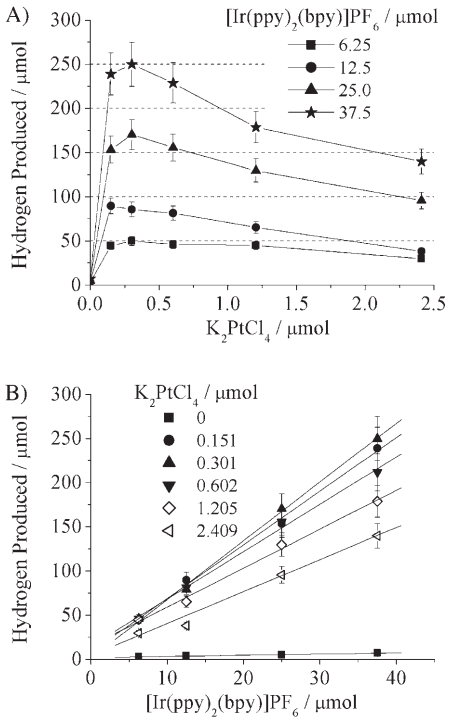

Figure 2. A) Net hydrogen produced after 20 h of illumination as a function of $[K_2PtCl_4]$ for a series of [PS]. Maximum hydrogen evolution occurs for a given [PS] when 0.301 μmol K_2PtCl_4 is added. B) Net hydrogen as a function of [PS] for a series of $[K_2PtCl_4]$. Linear fits of H_2 as a function of [PS] give $R^2 > 0.98$ for all nonzero K_2PtCl_4 concentrations and 0.96 when no K_2PtCl_4 is present.

To elucidate the mechanism of proton reduction, dynamic hydrogen evolution data were obtained for varying [PS].

Samples were monitored for hydrogen evolution by measuring the pressure as a function of time and correlating these plots to the final gas composition through GC analysis (Figure 3). The time-resolved hydrogen evolution data allow the determination of the reaction lifetime, and show that there is an induction period before the system starts to evolve hydrogen. The initial time required before hydrogen evolution starts may involve the formation of the active platinum catalyst from the K_2PtCl_4 salt, and usually lasts 1–3 minutes.

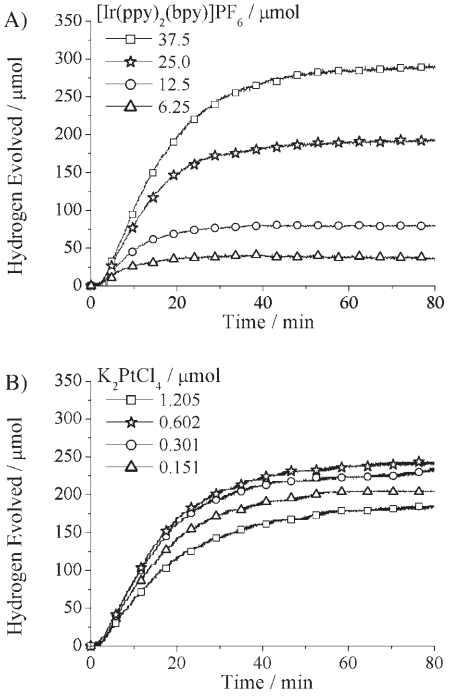

Figure 3. Photoreactions monitored in real time by pressure transducers. A) Series of four experiments where [PS] is varied each of which contains 0.301 μmol K_2PtCl_4. The initial rate, reaction decomposition time, and net hydrogen produced is affected by varying [PS]. B) Series of four experiments where $[K_2PtCl_4]$ is varied each of which contains 25.0 μmol PS. Varying $[K_2PtCl_4]$ shows a less dramatic effect on initial rate, decomposition time and net hydrogen produced.

Similar to the 20 h net hydrogen experiments, the total amount of hydrogen produced during the reaction is linearly related to the amount of PS added. In addition, the time elapsed before catalytic activity decays is clearly dependent on [PS]. Assuming that the rate of the reaction decreases due to the first-order decay of a rate-limiting reagent, net hydrogen production after the induction period was fit to a time-dependent function [Eq. (1)]:

$$H_2(t) = \alpha(1-e^{-t/\tau}) \quad (1)$$

where α is the net hydrogen produced, and τ is the decay lifetime for the rate of hydrogen evolution. This fit gives a good representation of the experimental data after the induction period. Both parameters (α and τ) were found to be strongly correlated to the initial [PS] (Figure 4A) but not to $[K_2PtCl_4]$ (Figure 4B). The optimal $[K_2PtCl_4]$ was found to be independent of [PS], and was determined by maximizing the α parameter for varying $[K_2PtCl_4]$. Increasing [PS] by a factor of 4 augments τ by a factor of 2.3, while raising $[K_2PtCl_4]$ by a factor of 8 only increases τ by a factor of 1.3. Such behavior strongly suggests first- or pseudo-first-order kinetics for the deterioration of PS.

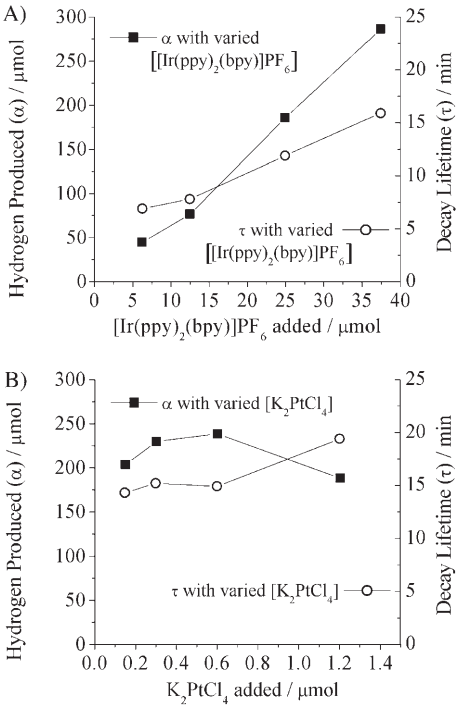

Figure 4. Best-fitting parameters α (net hydrogen produced) (left axis) and τ (right axis) from the first-order kinetic decomposition of the reaction rate giving the formula $H_2(t) = \alpha(1-e^{-t/\tau})$, plotted as functions of A) [PS] and B) $[K_2PtCl_4]$. K_2PtCl_4 (0.301 μmol) was added to the experiments where [PS] is varied, and PS (25.0 μmol) was added to the experiments where $[K_2PtCl_4]$ was varied.

ESI-MS data collected from the reaction mixture during the first hour of illumination clearly reveal the degradation of the PS ($[M]^+ = 657$) by 2,2′-bipyridine dissociation, which directly corresponds to decreased catalytic activity (Figure 5) (see Supporting Information for a similar study showing PS decomposition by UV/Vis spectroscopy). The observed loss of 2,2′-bipyridine from the $[Ir(ppy)_2(bpy)]^+$ complex eliminates the ^{3}MLCT excited state ($t_{2g} \rightarrow \pi^*_{N\wedge N}$) and limits excitations to those involving the LC transitions on the cyclometalating ligands. The excited state of the photoproducts therefore lack the charge separation of the original PS and are consequently inactive.

In an effort to regenerate the original PS, 2,2′-bipyridine (0.5 mmol) was added to a sample containing PS (25 μmol) and K_2PtCl_4 (0.301 μmol), which demonstrated a decreased catalytic activity and only produced 40% as much hydrogen

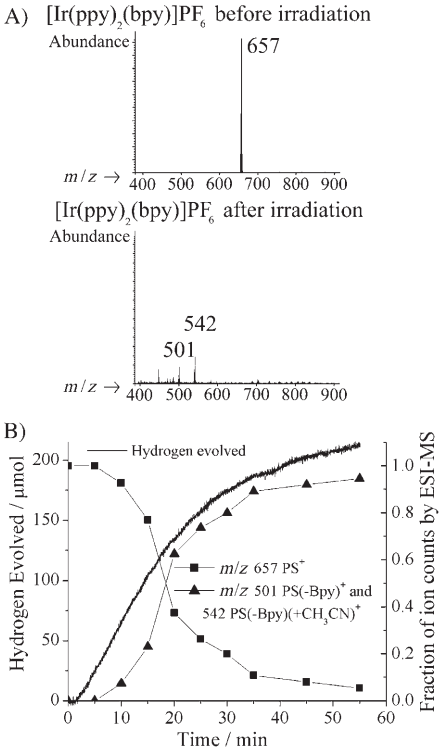

Figure 5. A) ESI-MS of $[Ir(ppy)_2(bpy)]PF_6$ before and after 20 h of irradiation showing the complete conversion of the PS $[M]^+$ ion (*m*/*z* 657) into the decomposition products $[Ir(ppy)_2]^+$ (*m*/*z* 501) and $[Ir(ppy)_2CH_3CN]^+$ (*m*/*z* 542). B) Fraction of PS present (right axis, squares) and decomposition products (right axis, triangles) as determined by ESI-MS from aliquots of a reaction containing PS (25.0 μmol) and K_2PtCl_4 (0.301 μmol) overlaid with the net hydrogen produced (left axis, solid line) from the system. The rate of hydrogen evolution decreases along with the presence of the $[M]^+$ ion. During the course of the reaction, PS decomposition peaks for $[Ir(ppy)_2]^+$ (*m*/*z* 501) and $[Ir(ppy)_2CH_3CN]^+$ (*m*/*z* 542) increase, thus indicating 2,2′-bipyridine dissociation.

as the system without added 2,2′-bipyridine. This loss in catalytic activity may be attributable to poisoning of the platinum catalyst.

To better understand the factors influencing the maximum hydrogen production, K_2PtCl_4, PS, or a combination of both PS and K_2PtCl_4 were added after each respective reaction had reached its pressure plateau. The lone addition of K_2PtCl_4 gave no increase in hydrogen production, while the addition of PS, or both species simultaneously, caused the headspace pressure to resume its climb in a similar fashion. However, the reaction conditions were not completely regenerated in that the performance of the catalytic system, even with a second addition of TEOA, was shorter lived and had a decreased turnover rate. Clearly, the PS becomes deactivated within a few hours of illumination, and after the catalytic species have decomposed, conditions have changed such that the system cannot be restored by the addition of K_2PtCl_4. One possible explanation is that the surface of the platinum catalyst is being quickly poisoned by the decomposition products of the reaction.

Colloidal platinum: To show that the active catalyst was a platinum metal colloid and to prevent aggregation, the catalyst source was modified to 8–10 nm presynthesized and surface-stabilized colloids.[38] As shown in Figure 6, this platinum source evolves hydrogen at a similar rate to the K_2PtCl_4 precursor, but significantly increases net hydrogen production by sustaining catalytic activity. Although the overall productivity of the system is dramatically increased, this system is extremely sensitive to the catalyst preparation and ripening. As a consequence, most studies described herein utilize the K_2PtCl_4 precursor to minimize fluctuations in the catalytic activity of the platinum colloid.

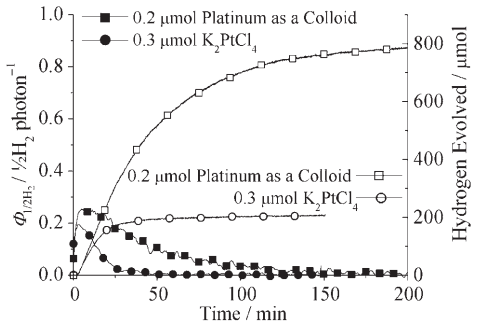

Figure 6. Real-time hydrogen evolution data using PS (25.0 μmol) and either a colloidal platinum or K_2PtCl_4 catalyst (right axis, open symbols). Quantum yield of hydrogen evolution ($\Phi_{1/2H_2}$) for both systems (left axis, solid symbols).

Through the use of a presynthesized and stabilized colloidal catalyst, turnover numbers of 63 are achieved for the $[Ir(ppy)_2(bpy)]PF_6$ photosensitizer, which corresponds to a 4.2-fold increase in production. Both systems have similar initial rates but the stabilized colloidal system is catalytically active for an extended time period. This is also demonstrated in the time-resolved quantum yield of hydrogen production ($\Phi_{1/2H_2}$, [Eq. (2)]) determined from the photon flow of the LED (Φ_p) that is calculated using its 500 mW power output and 465 nm average wavelength. $\Phi_{1/2H_2}$ reaches a maximum after only 5 minutes in both systems, but takes approximately 120 minutes longer to decay in the stabilized colloidal platinum system.

$$\text{photons absorbed} = (\Phi_p)(\Delta t)(1-10^{-\varepsilon cb})$$
$$(\varepsilon = 880\ \text{M}^{-1}\ \text{cm}^{-1};[17]\ c = 25.0\ \mu\text{mol}/9.75\ \text{mL};\ \text{and}\ b = 1.8\ \text{cm}) \quad (2)$$
$$\Phi_{1/2H_2} = 2\ (H_2\ \text{produced})/\text{photons absorbed}$$

By stabilizing the 8–10 nm particle size of the platinum catalyst, the rate of catalyst deactivation is reduced, which implies that PS decomposition is also slowed. We believe that the enhanced stability of this system comes from its extended capacity to oxidize the unstable PS^- back to the ground state PS. In contrast, when the unstabilized catalyst aggregates, its total surface area dramatically decreases and collisions between the catalyst and PS^- become infrequent, lead-

ing to a greater incidence of PS^- decomposition. This supposition also explains the increased catalytic efficiency of the stabilized colloid.

Mechanism of hydrogen evolution: To determine the source of the reduced protons, D_2O was used in place of H_2O in the 9:3:1 acetonitrile/water/TEOA reaction media, which resulted in a final gas composition of 64% D_2, 29% HD, and 7% H_2. It is therefore believed that the predominant mechanism is the direct reduction of protons from water using reductive equivalents transferred from TEOA to the platinum catalyst by the PS. Although the presence of H_2 and HD may in part be due to H_2O contamination of the other solvents in the system, their presence may also indicate that the TEOA is being used as a proton source in a secondary and less significant mechanism.

It is extremely important to note that, compared to the commonly studied tris-diimine Ru^{II} complexes, $[Ir(ppy)_2(bpy)]^+$ in its triplet excited state is much more inclined to undergo reductive electron transfer with TEOA.[17] Surprisingly, the relevant excited state redox property $E^{\circ\prime}$* $M^{n+}/M^{(n-1)+}$ is +0.68 V for both complexes[17] and the thermodynamics of an electron transfer from TEOA are identical. The variation in quenching behavior might arise from differences in the reorganization energy for electron transfer or from the electronic coupling of the outer sphere processes. DFT calculations on the triplet excited state were performed to understand the differences between Ru^{II}- and Ir^{III}-based photosensitizers. As expected, the LSUMO (lowest singly unoccupied molecular orbital) of the Ru^{II}-based sensitizer is exclusively (95 percentile) located on the d_{z^2} metal orbital that is surrounded with the inactive ligand framework, obstructing donor–acceptor orbital overlap and, as a consequence, renders electron transfer from a sacrificial reductant difficult (Figure 7). In contrast, the LSUMO of $[Ir(ppy)_2(bpy)]^+$ involves both, the d orbitals of the central ion as well as the π orbitals of the 2-phenylpyridine ligands, which facilitates reductive electron transfer reactions and increases the spatial separation of the charges in the excited state. For comparison, the HSOMO (highest singly occupied molecular orbital) of $[Ru(bpy)_3]^{2+}$ and $[Ir(ppy)_2(bpy)]^+$ are located exclusively on the 2,2′-bipyridine ligand(s).

Accordingly, a dual pathway mechanism is conceivable for photocatalytic proton reductions with $[Ir(ppy)_2(bpy)]^+$ derivatives as photosensitizers (Figure 8A) when an electron relay is present. The higher observed quantum efficiencies of the Ir^{III}-based systems compared to those for the Ru^{II} complexes, each with a $[Co(bpy)_3]^{2+}$ electron relay, are a clear indication of these mechanistic differences.[17] The fact that hydrogen evolution occurs without an electron relay implies that the reduced Ir^{III} complex is not only formed, but is also capable of reducing protons in the presence of a Pt colloid, as depicted in Figure 8B.

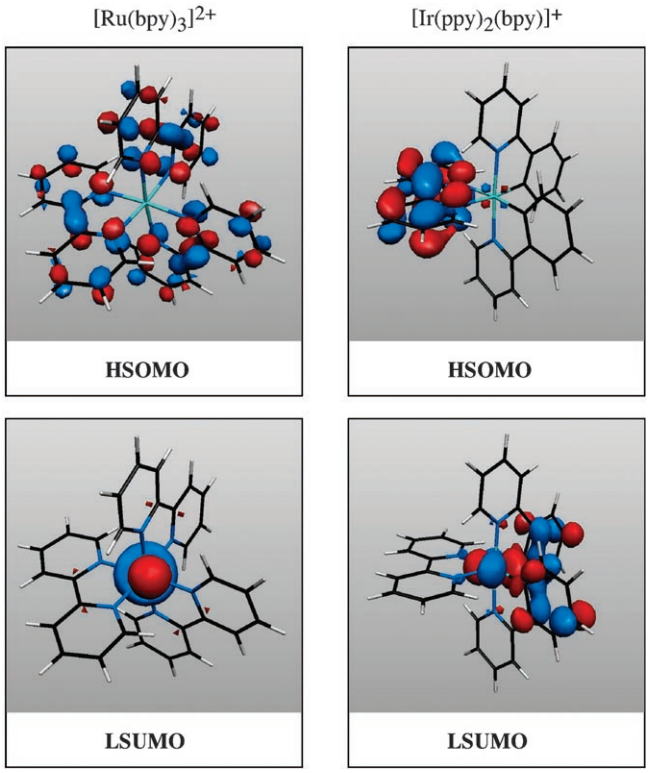

Figure 7. Frontier orbitals of $[Ru(bpy)_3]^{2+}$ (left) and $[Ir(ppy)_2(bpy)]^+$ (right) in the triplet excited state obtained through DFT calculations (B3LYP/LANL2DZ). The character of the LSUMO (lowest singly unoccupied molecular orbital) varies dramatically between the Ru^{II} and the Ir^{III} complex: While it is exclusively metal-based in $[Ru(bpy)_3]^{2+}$ (95 percentile), a mixed orbital of the Ir^{III} 5d orbital with the ppy ligand is observed for the Ir^{III} PS. The HSOMO of both complexes is exclusively localized on the bpy ligand(s).

Conclusion

A visible light driven catalytic water reduction system, comprising of only a $[Ir(ppy)_2(bpy)]PF_6$ photosensitizer, colloidal platinum, and sacrificial reductant, is capable of achieving up to 63 turnovers and reaches a maximum quantum yield for hydrogen production of 0.26. Elimination of the electron relay species removes any energy losses or back reactions associated with charge transfer to the relay, while making the system easier to study and optimize. Dissociation of the 2,2′-bipyridine ligand from the PS was observed by ESI-MS as the major pathway of decomposition. Time-resolved kinetic data obtained from pressure transducers provided insight into the reaction's lifespan and the effect of replenishing various components of the system. The overall mechanism of hydrogen evolution is discussed, involving reductive quenching of PS* followed by electron transfer to a proton-absorbing catalyst. The utilization of a reductively quenched PS* circumvents the need for an electron relay species and work is currently underway to couple this system to an oxygen evolving cycle with the ultimate goal of constructing a complete visible light driven water-splitting device.

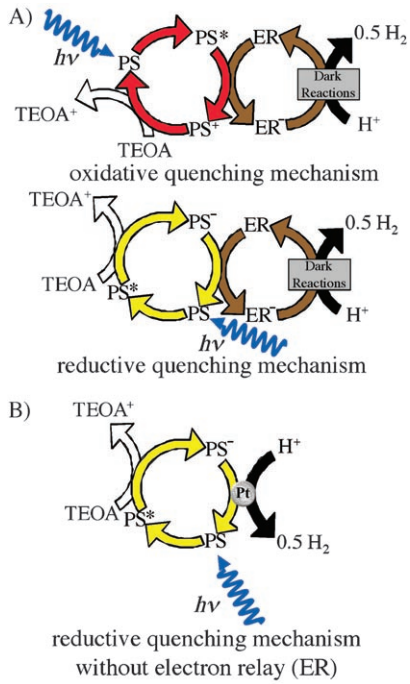

Figure 8. A) A dual pathway mechanism through an oxidative and a reductive quenching mechanism is possible with the $[Ir(ppy)_2(bpy)]^+$ sensitizer for the photoreduction of water. B) The presence of a reductive quenching mechanism allows the photoreduction to occur in absence of an electron relay complex.

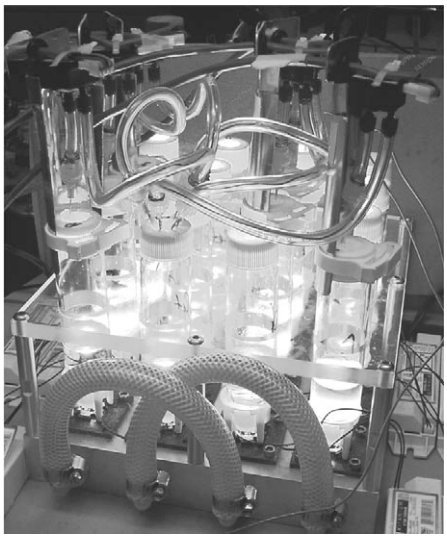

Figure 9. A 16-well LED photoreactor equipped with pressure transducers for time-resolved parallel sample analysis. The LEDs have an output of (500±50) mW and are mounted on a water-cooled aluminum block that is placed on an orbital shaker.

Experimental Section

General: ^{1}H NMR spectra were recorded on a Varian Inova-500 spectrometer at room temperature. Mass Spectra (MS) were obtained using a Hewlett-Packard Electrospray (ESI) MS engine. Gas chromatograph (GC) analysis for H_2 was performed on a Perkin–Elmer 3920 chromatograph with a 13x 80/100 mesh molecular sieve column (Alltech), thermal conductivity detector, and an argon carrier gas. H_2 production was quantified from a calibration of H_2/N_2 mixtures, and verified by bracketing each set of samples with injections containing known points from the calibration curve.

Synthesis: The $[Ir(ppy)_2(bpy)]PF_6$ complex was synthesized and characterized as previously described[39] and recrystallized by vapor diffusion from acetonitrile/diethyl ether. All other solvents and reagents are commercially available and were used without further purification.

20 hour net hydrogen evolution experiments: Samples were prepared in 40 mL pre-cleaned screw cap vials (VWR) with silicone/PTFE septa from 750 μL of a 8.33×10^{-3} M, 1.67×10^{-2} M, 3.33×10^{-2} M, or 5.00×10^{-2} M PS stock solution in acetonitrile and a 9:3:1 acetonitrile/water/TEOA solution (9.0 mL). To this solution was added 10 to 100 μL of an aqueous K_2PtCl_4 solution. Samples were capped and deoxygenated by bubbling N_2 into the solution for 30 min, after which any dissolved N_2 was removed by placing the sample under a dynamic vacuum for 30 min. The samples were then placed in a home-built, 16 sample photoreactor (Figure 9) illuminated from the bottom using LEDs at 465 nm with a 20 nm FWHM (Luxeon V Dental Blue, Future Electronics) with collimating optics (Fraen, FHS-HNB1-LL01-H) to give a total output power of (500± 50) mW. The LEDs are driven at 700 mA using a Xitanium Driver (Advance Transformer Company) and are fixed to a copper plate that is situated on a water cooled aluminum block. The entire setup is agitated at 150 rpm using an orbital shaker (IKA, KS 260). After 20 h of illumination, the samples were backfilled with water, bringing the head space to ambient pressure. Analysis of gases were performed using a Hamilton SampleLock syringe and either a calibrated hydrogen sensor as previously described,[17] or by GC when head space volumes did not exceed 2 mL.

Time-resolved hydrogen evolution measurements: For real-time characterization of hydrogen evolution, samples were prepared in the manner of the experiments described above. The degassing procedure was modified such that deoxygenation occurred through seven iterations of a 1 min evacuation followed by backfilling with nitrogen. In preliminary studies, hydrogen evolution was monitored by bubbling the overpressure into a water-filled burette and then analyzing the resulting gas mixture by GC. This procedure was further automated through the use of temperature-compensating differential pressure transducers (Omega, PX-138-015D5V). Pressure readings were corrected for the heating of the solution by connecting the transducer to the sealed sample vial and a reference vial containing acetonitrile (750 μL) and the 9:3:1 acetonitrile/water/TEOA solution (9.0 mL). The transducers have an operating range of ±15 psi, an accuracy of ±0.015 psi, and are driven in parallel at 8 V using a variable power supply (Temna 72–2005). Pressure data were collected every 250 ms from eight samples using a PC interface designed in LabView. Approximately 2 h after the pressure reached a static value (typically within 3 h of illumination), the samples were brought to ambient pressure by bubbling into a water-filled burette, and the resulting gas was analyzed by GC to correlate hydrogen production to the observed pressure increase.

D_2O experiment: A 3.33×10^{-2} M PS solution (750 μL) in CH_3CN was combined with a 9:3:1 acetonitrile/D_2O (Cambridge, 99.9% D)/TEOA solution (9.0 mL) and a 0.0301 M aqueous K_2PtCl_4 solution (10 μL). The sample was evacuated and subsequently illuminated for 2 h, after which the resulting gas was brought to atmospheric pressure by backfilling with water. The resulting headspace was then leaked through a valve (PSV, Aalborg) into a UHV chamber (evacuated by Pfeiffer PMS03525) and analyzed by a Residual Gas Analyzer (RGA300, Stanford Research Systems)

Colloidal platinum experiments: Colloidal platinum (8–10 nm) stabilized by sodium polyacrylate[38] was synthesized in water to give an approximate Pt loading of 0.02 mg Pt/mL. Samples were then prepared using a $3.33x10^{-2}$ M PS stock solution (750 μL), the platinum colloid (2.0 mL), and a 9:1 acetonitrile/TEOA solution (7.0 mL), to give similar reaction conditions to the K_2PtCl_4 experiments.

DFT calculations: DFT calculations (B3LYP/LANL2DZ) were performed by using Gaussian 03.[40]

Acknowledgements

The authors thank Paul W. Majsztrik for his conversations regarding the development of the time-resolved apparatus. S.B. gratefully acknowledges support from a Camille and Henry Dreyfus New Faculty Award and a NSF CAREER award (CHE-0449755).

[1] O. Khaselev, J. A. Turner, *Science* **1998**, *280*, 425–427.
[2] Z. Zou, J. Ye, K. Sayama, H. Arakawa, *Nature* **2001**, *414*, 625–627.
[3] M. Grätzel, *Nature* **2001**, *414*, 338–344.
[4] J. S. Lee, *Catal. Surv. Jpn.* **2005**, *9*, 217–227.
[5] A. Steinfeld, *Solar Energy* **2005**, *78*, 603–615.
[6] E. Amouyal in "Water Splitting: from Molecular to Supramolecular Photochemical Systems" *Homogenous Photocatalysis, Vol. 2* (Ed.: M. Chanon), Wiley, Chichester, **1997**, pp. 263–308.
[7] J. Kiwi, E. Borgarello, E. E Pelizzett, M. Visca, M. Grätzel in "H_2 Evolution Induced by U.V. and Visible Light in Cyclic Processes via H_2O Cleavage" *Photogeneration of Hydrogen*, (Eds.: A. Harriman and M. A. West), Academic Press, London, **1982**, pp. 119–146.
[8] J.-M. Lehn, J. P. Sauvage, *Nouv. J. Chim.* **1977**, *1*, 449–451.
[9] A. Moradpour, E. Amouyal, P. Keller, H. Kagan, *Nouv. J. Chim.* **1978**, *2*, 547–549.
[10] M. Grätzel, *Acc. Chem. Res.* **1981**, *14*, 376–384.
[11] D. Duonghong, E. Borgarello, M. Grätzel, *J. Am. Chem. Soc.* **1981**, *103*, 4685–4690.
[12] J. R. Darwent, P. Douglas, A. Harriman, G. Porter, M. C. Richoux, *Coord. Chem. Rev.* **1982**, *44*, 83–126.
[13] L. Persaud, A. J. Bard, A. Campion, M. A. Fox, T. E. Mallouk, S. E. Webber, J. M. White, *J. Am. Chem. Soc.* **1987**, *109*, 7309–7314.
[14] E. Adar, Y. Degani, Z. Goren, I. Willner, *J. Am. Chem. Soc.* **1986**, *108*, 4696–4700.
[15] Y. Tomonou, Y. Amao, *BioMetals* **2003**, *16*, 419–424.
[16] N. Sugiyama, M. Toyoda, Y. Amao, *Colloids Surf. A* **2006**, *284–285*, 384–387.
[17] J. I. Goldsmith, W. R. Hudson, M. S. Lowry, T. H. Anderson, S. Bernhard, *J. Am. Chem. Soc.* **2005**, *127*, 7502–7510.
[18] M. S. Lowry, J. I. Goldsmith, J. D. Slinker, R. Rohl, R. A. Pascal, G. G. Malliaras, S. Bernhard, *Chem. Mater.* **2005**, *17*, 5712–5719.
[19] K. Kalyanasundaram, *Photochemistry of Polypyridine and Porphyrin Complexes*, Academic Press, New York, NY, **1992**, p. 105–164.
[20] R. J. Watts, J. Van Houten, *J. Am. Chem. Soc.* **1974**, *96*, 4334–4335.
[21] M. G. Colombo, A. Hauser, H. U. Güdel, *Inorg. Chem.* **1993**, *32*, 3088–3092.
[22] M. G. Colombo, A. Hauser, H. U. Güdel, *Top. Curr. Chem.* **1994**, *171*, 143–171.
[23] P. J. Hay, *J. Phys. Chem. A* **2002**, *106*, 1634–1641.
[24] E. Amouyal, B. Zidler, P. Keller, A. Moradpour, *Chem. Phys. Lett.* **1980**, *74*, 314–317.
[25] E. Amouyal, B. Zidler, *Isr. J. Chem.* **1982**, *22*, 117–124.
[26] C. V. Krishnan, N. Sutin, *J. Am. Chem. Soc.* **1981**, *103*, 2141–2142.
[27] C. V. Krishnan, B. S. Brunschwig, C. Creutz, N. Sutin, *J. Am. Chem. Soc.* **1985**, *107*, 2005–2015.
[28] J. Hawecker, J. M. Lehn, R. Ziessel, *Nouv. J. Chim.* **1983**, *7*, 271–277.
[29] G. M. Brown, S. F. Chan, C. Creutz, H. A. Schwarz, N. Sutin, *J. Am. Chem. Soc.* **1979**, *101*, 7638–7640.
[30] S. F. Chan, M. Chou, C. Creutz, T. Matsubara, N. Sutin, *J. Am. Chem. Soc.* **1981**, *103*, 369–379.
[31] M. Kirch, J. M. Lehn, J. P. Sauvage, *Helv. Chim. Acta* **1979**, *62*, 1345–1384.
[32] H. Ozawa, M. Haga, K. Sakai, *J. Am. Chem. Soc.* **2006**, *128*, 4926–4927.
[33] S. Rau, B. Schäfer, D. Gleich, E. Anders, M. Rudolph, M. Friedrich, H. Görls, W. Henry, J. G. Vos, *Angew. Chem. Int. Ed.* **2006**, *45*, 6215–6218.
[34] M. Falkenström, O. Johansson, L. Hammarström, *Inorg. Chim. Acta* **2007**, *360*, 741–750.
[35] S. Ott, M. Kritikos, B. Åkermark, L. Sun, *Angew. Chem. Int. Ed.* **2003**, *42*, 3285–3288.
[36] P. J. DeLaive, B. P. Sullivan, T. J. Meyer, D. G. Whitten, *J. Am. Chem. Soc.* **1979**, *101*, 4007–4008.
[37] J. Kiwi, M. Grätzel, *Nature* **1979**, *281*, 657–658.
[38] T. S. Ahmadi, Z. L. Wang, T. C. Green, A. Henglein, M. A. El-Sayed, *Science* **1996**, *272*, 1924–1926.
[39] M. S. Lowry, W. R. Hudson, R. A. Pascal, S. Bernhard, *J. Am. Chem. Soc.* **2004**, *126*, 14129–14135.
[40] Gaussian 03, Revision C.02, M. J. Frisch, G. W. Trucks, H. B. Schlegel, G. E. Scuseria, M. A. Robb, J. R. Cheeseman, J. A. Montgomery, Jr., T. Vreven, K. N. Kudin, J. C. Burant, J. M. Millam, S. S. Iyengar, J. Tomasi, V. Barone, B. Mennucci, M. Cossi, G. Scalmani, N. Rega, G. A. Petersson, H. Nakatsuji, M. Hada, M. Ehara, K. Toyota, R. Fukuda, J. Hasegawa, M. Ishida, T. Nakajima, Y. Honda, O. Kitao, H. Nakai, M. Klene, X. Li, J. E. Knox, H. P. Hratchian, J. B. Cross, V. Bakken, C. Adamo, J. Jaramillo, R. Gomperts, R. E. Stratmann, O. Yazyev, A. J. Austin, R. Cammi, C. Pomelli, J. W. Ochterski, P. Y. Ayala, K. Morokuma, G. A. Voth, P. Salvador, J. J. Dannenberg, V. G. Zakrzewski, S. Dapprich, A. D. Daniels, M. C. Strain, O. Farkas, D. K. Malick, A. D. Rabuck, K. Raghavachari, J. B. Foresman, J. V. Ortiz, Q. Cui, A. G. Baboul, S. Clifford, J. Cioslowski, B. B. Stefanov, G. Liu, A. Liashenko, P. Piskorz, I. Komaromi, R. L. Martin, D. J. Fox, T. Keith, M. A. Al-Laham, C. Y. Peng, A. Nanayakkara, M. Challacombe, P. M. W. Gill, B. Johnson, W. Chen, M. W. Wong, C. Gonzalez, and J. A. Pople, Gaussian, Inc., Wallingford CT, **2004**.

Received: January 20, 2007
Revised: May 31, 2007
Published online: July 24, 2007

